Efficient silicon waveguide to plasmonic waveguide mode converter based on optimization algorithms

Tian Zhang, Zunwei Liu, Yihang Dan, Shuai Yu, Xu Han, Jian Dai, and Kun Xu

***Abstract*—We propose a novel mode converter based on the embedded coding metamaterials to effectively convert the TE/TM mode in a silicon waveguide to the SPPs mode in a plasmonic waveguide with high conversion efficiency and wide bandwidth. In order to improve the performance metrics, some optimization methods (genetic algorithm, particle swarm optimization, multi-traversal direct-binary search and simulated annealing) are applied in the design of coding metamaterials. The simulation results exhibit the converter can perform polarization-invariant conversion, and the conversion efficiency and bandwidth reach more than 0.93 and 200 nm, respectively. Compared with the previous results, we not only propose a high-performance mode converter but also introduce an efficient algorithm for inverse design of coding metamaterials.**

***Index Terms*—Mode converter, optimization, inverse design.**

I. INTRODUCTION

Surface plasmon polaritons (SPPs) is a special electromagnetic wave which can transmit on the interface between metal and dielectric [1-2]. Owing to breaking the diffraction limit, SPPs have been used to realize many photonic devices with compact dimension, such as plasmonic filter [3], splitter [4], switch [5], modulator [6], absorber [7], sensor [8], logic gate [9] and so on. In order to construct plamonic circuits, plasmonic mode converter (PMC), which converts the TE/TM mode in a silicon waveguide to the SPPs mode in a plasmonic waveguide, has been an active research topic because it's a fundamental photonic device in the optical interconnection system [10-14]. Recently, a great deal of plasmonic waveguide structures, such as metallic slot waveguide and metal-dielectric-metal (MDM) waveguide, have been used to design various PMCs for adapting different integrated environment [10]. For these PMCs, conversion efficiency and bandwidth are two critical performance metrics. For example, it had been proven that the conversion efficiency and 1 dB bandwidth of an early proposed PMC reached to 85% and 200 nm, respectively [11]. And a directional PMC was specially designed to achieve polarization-invariant coupling with high conversion efficiency [12]. In order to increase conversion efficiency, the traditional straight waveguide in the PMC was replaced with a slot-taper structure for gradually squeezing the TE/TM mode from the silicon waveguide into the plasmonic waveguide [13]. In addition to the ingenious design of device structure, some optimization algorithms had been used to search for the appropriate structure parameters of the slot-taper [14]. However, the optimization abilities were limited because it only optimized for a specific taper structure rather than a relatively complete optimization space. And there were few polarization-invariant PMC had high conversion efficiency and wide bandwidth simultaneously. It's expected to further improve conversion efficiency and bandwidth by designing ingenious device structure and selecting effective optimization algorithms.

In general, inverse design and performance optimization of the photonic devices can be solved by using three methods, namely gradient based methods, gradient free methods and model based methods [15-16]. As a representative method of the gradient based methods, adjoint variable method (AVM) can optimize for the linear and nonlinear optical devices, but it needs physical background to derive the gradient of objective function [17]. Apart from the gradient-based methods, model based methods, such as artificial neural networks and random forest, are also used to inversely design the photonic devices [16, 18]. However, in order to train the model whose inputs are physical parameters and outputs are electromagnetic response, it requires a significant amount of time to generate the training instances and test instances [16]. Compared with the gradient based methods and model based methods, the gradient free methods which depends on search strategy and evolutionary strategy are simple and effective [15]. Genetic algorithm (GA) and particle swarm optimization (PSO) are representative evolutionary algorithms which are inspired by the biological evolution and natural selection [15]. It should be noted that the convergent speed of the evolutionary algorithm are relatively slow because they need to control the population consisted of individuals. And simulated annealing (SA) and direct-binary search (DBS) are typical search algorithms which require less time to converge [19]. But the finite traversal times (usually only once) restrict the optimization ability of the DBS.

In this paper, we propose a novel mode converter based on the embedded coding metamaterials. And several optimization algorithms are used to design the coding metamaterials to improve the performance metrics of PMC. Compared with the PMC optimized by GA, PSO and SA, the simulated results show that the PMC optimized by multi-traversal DBS can simultaneously achieve high conversion efficiency (>0.93) and wide bandwidth (>200 nm).

Manuscript received XXX, 2019; revised XXX, 2019; accepted XXX, 2019. This work was supported by the National Natural Science Foundation of China under Grants 61625104 and 61431003, the Beijing Municipal Science & Technology Commission under Grants Z181100008918011, the Ministry of Science and Technology of China under Grants 2016YFA0301300, the Fundamental Research Funds for the Central Universities under Grants 2019RC15 and 2018XKJC02.

T. Zhang, Z. Liu, Y. Dan, S. Yu, J. Dai, K. Xu are with State Key Laboratory of Information Photonics and Optical Communications, Beijing University of Posts and Telecommunications, Beijing 100876, P.R. China (e-mail: xukun@bupt.edu.cn).

X. Han is with Huawei Technologies Co., Ltd, Shenzhen 518129, Guangdong, China

Color versions of one or more figures in this paper are available online at http://ieeexplore.ieee. org.

II. Device Design and Simulation Results

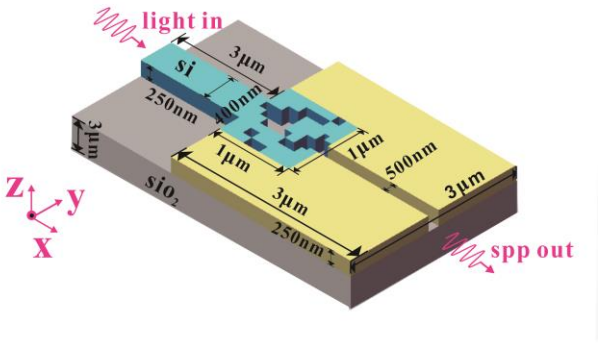

Fig.1 Structure schematic of the proposed PMC.

As shown in Fig.1, we propose a PMC which consists of a silicon waveguide, silicon-based coding metamaterials (SCM) and a plasmonic MDM waveguide. All waveguides and SCM are placed on a silica substrate with the thickness of 3 μm. Here, the SCM whose footprint is 1×1 μm^2 and composition is M×N square pixels are embedded into the metal (Au). Each pixel in the SCM can be selectively filled by silicon or air, corresponding to the logical "1" or "0" state, respectively. Obviously, the SCM provides a relatively broad optimization space compared with the specific device structure in [14]. The length, width and height of the input silicon waveguide which transmits the TM/TE mode polarized light are 3 μm, 0.4 μm and 0.25 μm, respectively. The TM/TE modes in the silicon waveguide are converted to the plasmonic modes by the SCM. After that, the plasmonic modes are coupled into the MDM waveguide whose length and width are 2 μm and 0.05 μm, respectively. In our simulation, the transmission spectrum of the PMC is calculated by the 2.5-dimensional finite-difference time-domain (FDTD) method (adopting Lumerical MODE Solutions). The metal in the FDTD simulation is modeled by the Drude model with (ε_∞, ω_p, γ_p) = (3.7, 9.1 eV, 0.018 eV) [16]. The conversion efficiency of PMC is defined as the ratio of the power coupled into the plasmonic waveguide and the output power of the silicon waveguide. It should be noticed that the transmission loss of the MDM waveguide is calculated by placing several monitors in the waveguide.

First of all, we use two evolutionary algorithms (GA and PSO) and one search algorithm (SA) to design and optimize the PMC. As typical gradient free methods, GA and PSO have been applied in optimizing for various photonics devices due to their simplicity and effectiveness [15]. The algorithmic details of GA are outlined as follows: (i) randomly generating an initial population consisted of N=50 individuals. Here, each individual in the initial population is the SCM whose pixels are randomly initialized as "1" or "0" state. (ii) For all N SCMs, the transmission spectrums are calculated by using the FDTD method. The difference between simulated transmission spectrum and targeted transmission spectrum (all the transmittances in wavelength range 1.5 μm ~1.6 μm are 1) is defined as the optimization objective (fitness) for GA. (iii) Trying to generate a new population by using the selection, crossover and mutation procedures. In the selection process, two parent individuals are selected from previous generation based on the roulette-wheel selection with gap selection ratio 0.8 [16]. Here, the SCM with smaller difference are selected with higher probability. In the crossover process, the selected SCMs cross over to generate a new SCM based on the uniform crossover method with a crossover probability of 0.3. In the mutation process, each pixel in the SCM has 5% probability to flip from 0 (1) to 1 (0). (iv) The newly generated SCMs are evaluated to determine the GA whether to stop or not. If the genetic generation reaches to 100 or the difference remain unchanged for more than 5 times, then GA stops, otherwise, proceeds to Step (ii). Compared with GA, PSO is an evolutionary algorithm which is suitable for the decimal rather than binary number [20]. For PSO, the individuals (SCMs) in a population depend on the globally optimal individual and historically optimal record for each individual to search for optimal solution [20]. It should be noticed that the discrete binary PSO (DBPSO) rather than the standard PSO is used to optimize the SCM. In the DBPSO, the calculation method for the velocity is as same as the standard PSO. But the velocity of the standard PSO directly affects the position of particle, while that of DBPSO is converted to a flip probability based on the sigmoid function [21]. Then, this flip probability determines whether the pixels in SCMs are changed or not. The speed range, inertia weight and acceleration constants of the DBPSO in this article are set as -1~1, 1, and c_1=c_2=1.49, respectively. Moreover, SA is a typical search algorithm which imitates the physical annealing in the quenching whose molecules tend to a stable state as temperature decreases [19]. At the initial stage, SA searches for the solution in a broad optimization space by accepting a worse solution with a certain probability. It can alleviate the local optima problem to some extent [19]. As the temperature decreases, the solution changes in a small range to speed up the convergence of SA. Here, in each iteration, SCM is randomly generated and simulated by using the FDTD method. The objective function (difference) is evaluated to determine the newly generated SCM whether to accept with a acceptance probability determined by the Metropolis criterion [22]. Here, the maximum and minimum of the temperature for the SA are set as 2000 and 1e^{-18}, respectively.

We use GA, DBPSO and SA to optimize the PMC when the SCM is composed of 40×40 pixels, and the calculated results are shown in Fig. 2. The transmission spectrums of the PMCs whose SCMs are randomly initialized for GA, DBPSO and SA are exhibited in Fig. 2(a). Before the optimization, we observe that the transmittances in wavelength range 1.50 μm ~1.60 μm are very low and the maximum of the transmittances is lower than 0.30, indicating the PMC is ineffective because of the small conversion efficiency. In order to improve the coupling efficiency, GA, DBPSO and SA are applied in the optimization for PMC, and the variation of differences for different iterations are shown in Fig. 2(b) and Fig. 2(c). It can be found that the differences of GA, DBPSO and SA decrease from 83.2, 72.5, and 75.6 to 32.3, 35.7 and 27, respectively. And in the last iteration, the average absolute deviation for each point in the transmission spectrum are 32.3/100=0.323 (GA), 35.7/100=0.357 (DBPSO) and 27/100=0.27 (SA). Obviously, we can come to a conclusion that all optimization algorithms are convergent (effective) because the differences have sharp declines and the optimized transmission spectrums are close to the targeted transmission spectrum. This also can be confirmed by the calculated transmission spectrums before and after the optimization. In Fig. 2(d), all the transmittances

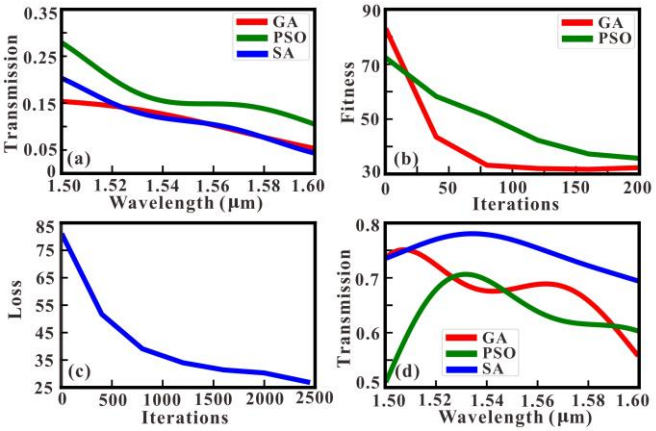

Fig.2 (a) The transmission spectrums of the PMCs whose SCMs are randomly initialized for GA, DBPSO and SA. (b) The variation of differences for GA and DBPSO in different iterations. (c) The variation of differences for SA in different iterations. (d) The simulated transmission spectrums after GA, DBPSO and SA optimizations.

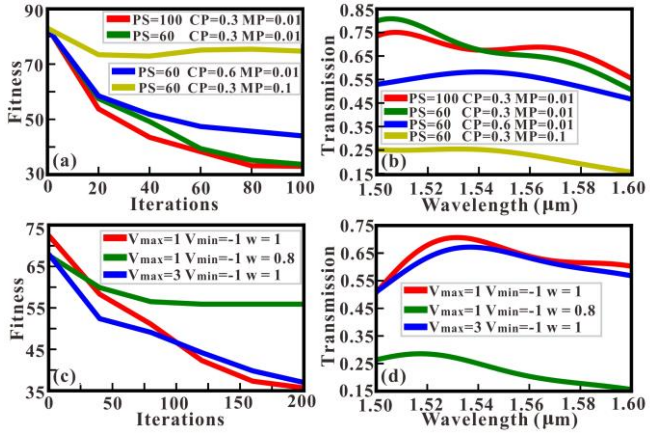

Fig.3 (a) The variation of differences for the GA with different optimization parameters. (b) After the optimization, the simulated transmission spectrums for different parameters of GA. (c) The variation of differences for DBPSO with different optimization parameters. (d) After the DBPSO optimization, the simulated transmission spectrums for different optimization parameters.

in the optimized transmission spectrums for GA, DBPSO and SA reach more than 50%, and the maximum transmittances for GA, DBPSO and SA are 0.75, 0.71 and 0.78 respectively. Finally, we consider the influences of parameter setting on the optimization results for GA and DBPSO. In Fig. 3(a), The variation of differences for different population sizes (PS), crossover probabilities (CP) and mutation probabilities (MP) of GA are calculated based on the FDTD method. It can be found that the fitness decreases from 33.7 to 33.0 when the population size increases from 60 to 100, indicating that the larger the population size is, the better the optimization result is. It's easy to explain that the large population size enhance the global searching ability of GA [16]. In addition, the increase of mutation probability may result in the performance degradation of PMC because a large mutation probability can cause instability and reduce the convergence speed of GA. Fig. 3(b) exhibits the optimized transmission spectrums for different parameter setting of GA. We can find that the large mutation probability and the small population size can reduce optimization effects of PMC. Similarly, Fig. 3(c) exhibits the variation of differences for different velocity ranges (V_{min} ~V_{max}) and inertia weights (w) of DBPSO. It can be found that the difference decreases from 55.9 to 35.7 when the inertia weight increases from 0.8 to 1. And we find that there is no linear correlation between the velocity range and difference. In general, the inertia weight and velocity range of DBPSO affect the attenuation speed and search scope in each iteration. And they both have influence on the convergence speed. Here, the decrease of inertia weight reduces the optimization effect of DBPSO because of the rapid attenuation speed. After the optimization, the simulated transmission spectrums (Fig. 3(d)) for different parameters also confirm this conclusion. In order to achieve rapid convergence, the variable inertia weight for different iterations can be employed in DBPSO. And the velocity range should be configured in a reasonable range to control the relationship between the convergence speed and search scope.

Next, a non-linear search algorithm, DBS, is used to design the distribution of SCM. The algorithmic details of DBS are outlined as follows: (i) the states "1" or "0" in the SCMs are randomly assigned for a specific PMC. Then, the transmission spectrum of the PMC is calculated by using the FDTD method. (ii) The state of the pixel which locates on some position flips from 0 (1) to 1 (0). Here, if the previous state is '0', it will be changed to '1' and vice versa. In this article, the change of the pixel is executed sequentially and row-wise. It means that if all pixels in the first row are executed, the pixels in the second row will be executed sequentially. Then, the PMC included newly generated SCM is simulated by using the FDTD method. After that, the sum of the transmittances in newly generated transmission spectrum is compared with that in previous transmission spectrum. If the sum of the current transmittances is higher than that of the previous transmittances, the newly generated SCM will be accepted. And the state of this pixel will not change when the sum of the current transmittances is smaller than that of previous transmittances. (iii) The condition of DBS is evaluated to determine the method whether to stop or not. In the traditional DBS, if the algorithm traverses all pixels in SCM once, then it stops, otherwise, proceeds to Step (ii). In order to further improve the algorithm searching ability, we propose a multi-traversal DBS (MDBS) to traverse SCM several times in succession. And we use the MDBS to optimize the SCM in PMC.

Fig. 4 exhibits the optimization results for the PMC by using the MDBS. Here, we consider three different densities (20×20, 30×30 and 40×40) for the SCM. The transmission spectrums of the PMCs whose SCMs are randomly initialized in the first iteration for three different densities are shown in Fig. 4(a). It can be found the maximums of the transmittances for three densities are lower than 0.20, indicating the PMC is ineffective when the SCMs are randomly initialized. We use the MDBS to optimize the SCM with 5 times complete traversals. And the optimization objective (the difference between the optimized transmission spectrum and targeted transmission spectrum) for different traversal times is shown in Fig. 4(b). It can be found that the optimization objectives have sharp declines from the beginning, indicating that the DBS is effective for the inverse design of the PMC. And the optimization results are close to those of GA, DBPSO and SA after the first traversal. In order to further reduce the difference, the MDBS is used to traverse the SCM for 4 times repeatedly. Surprisingly, the differences are further reduced for all SCMs with different densities. After five traversals, the average absolute deviation for each point in transmission spectrums are 5.73/100≈0.057, 5.79/100≈0.06

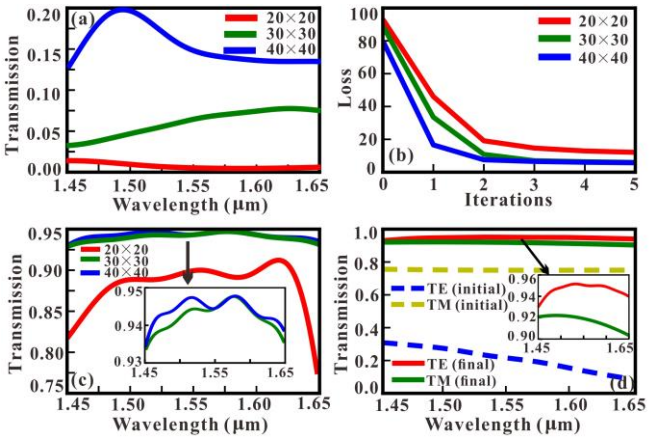

Fig.4 (a) The transmission spectrums of the PMCs whose SCMs are randomly initialized for different densities. (b) The variation of differences for different traversal times. (c) The optimized transmission spectrums for the SCMs with different densities after the fifth traversal. (d) The transmission spectrums of the PMC before the optimization (dash line) and after the optimization (solid line).

and 12.08/100≈0.12 for the SCMs with 40×40, 30×30 and 20×20, respectively. Obviously, the transmission spectrums of the PMCs optimized by the MDBS are closer to the targeted transmission spectrum than the optimized results by using GA, DBPSO and SA. After the fifth traversal, the optimized transmission spectrums also confirm this conclusion. It can be found in Fig. 4(c) that the optimized transmission spectrums for 40×40 and 30×30 SCMs are smooth and leveling out at around 0.94 in a wide bandwidth 200 nm, which is beneficial to the realization of wideband and efficient PMC.

Finally, the SCM is also optimized by using the MDBS to achieve the polarization-invariant PMC with high conversion efficiency and wide bandwidth simultaneously. To that end, the PMC in the FDTD simulation includes a 40×40 SCM and the traversal times of the MDBS is set as 5. Compared with the MDBS only for TM mode, the optimization objective here is adjusted to satisfy the high conversion efficiency regardless of TM mode or TE mode. Thus, the optimization objective of the MDBS is no longer the difference between the optimized transmission spectrum and targeted transmission spectrum for TM mode. The optimized transmission spectrum for TE mode is also considered here. In each iteration of MDBS, the FDTD simulation for PMC will be calculated twice: the first FDTD simulation is calculated for TM mode, and the second FDTD simulation is calculated for TE mode. Then, the differences between the targeted transmission spectrum and optimized transmission spectrum for TM mode and TE mode are added to comprehensively evaluate the performance of optimized SCM. If this value is reduced, the new SCM will be accepted, otherwise, it will be rejected. Fig. 4(d) shows the transmission spectrums of the PMC before the optimization (dash line) and after the optimization (solid line). It can be found that before the optimization of SCM, no matter which mode is inputted in the silicon waveguide, the transmittances in the transmission spectrum are small, meaning that TM/TE mode can hardly be converted to the SPPs mode in the plasmonic waveguide. And after the optimization of SCM, no matter TM mode and TE mode, the conversion efficiencies are improved and leveling out a high level (0.93 for TE and 0.91 for TM) in a wide bandwidth 200 nm, suggesting a polarization-invariant PMC is achieved by optimizing for SCM based on the MDBS.

III. CONCLUSION

In conclusion, we propose a novel PMC to effectively perform the mode conversion between the TE/TM mode in a silicon waveguide and the SPPs mode in a plasmonic waveguide. And several different optimization algorithms, such as GA, DBPSO, SA and DBS, are applied in the design of the SCM in the PMC to improve the performance metrics. The FDTD simulated results demonstrate that the PMC optimized by MDBS can perform polarization-invariant conversion, and the conversion efficiency and bandwidth reach more than 0.93 and 200 nm, respectively. Compared with previous articles, our proposed PMC designed by the optimization algorithms has superiority in conversion efficiency and bandwidth.

REFERENCES

[1] D.K. Gramotnev and S.I. Bozhevolnyi, "Plasmonics beyond the diffraction limit," Nat. Photonics 4, 83-91 (2010).
[2] T. Zhang, L. Chen, and X. Li, "Graphene-based tunable broadband hyperlens for far-field subdiffraction imaging at mid-infrared frequencies," Opt. Express 21, 20888-20899 (2013).
[3] H. Li and te al, "Investigation of the graphene based planar plasmonic filters," Appl. Phys. Lett. 103, 211104 (2013).
[4] T. Zhang, X. Yin, L. Chen, X. Chen, "Ultra-compact polarization beam splitter utilizing a graphene-based asymmetrical directional coupler," Opt. Lett. 41(2), 356-359 (2016).
[5] W. Chang and et al, "A plasmonic fano switch," Nano Lett. 12(9), 4977-4982 (2012).
[6] A. Melikyan and et al, "High-speed plasmonic phase modulators," Nat. Photonics 8, 229-233 (2014)..
[7] X. Xiong and et al, "Broadband plasmonic absorber for photonic integrated circuits," IEEE Photon. Techno. Lett. 26(17), 1726-1729 (2014).
[8] D. Rodrigo and et al, "Mid-infrared plasmonic biosensing with graphene," Science 349(6244), 165-168 (2015).
[9] T. Zhang and et al, "Plasmon induced absorption in a graphene-based nanoribbon waveguide system and its applications in logic gate and sensor," J. Phys. D: Appl. Phys. 51, 055103 (2018).
[10] Y. Fang and M. Sun, "Nanoplasmonic waveguides: towards applications in integrated nanophotonic circuits," Light-Sci Appl. 4, e294 (2015).
[11] A. Melikyan and et al, "Photonic-to-plasmonic mode converter," Opt. Lett., 39(12), 3488 (2014).
[12] J. Lin and et al, "Polarization-controlled tunable directional coupling of surface plasmon polaritons," Science, 340(6130), 331-334 (2013).
[13] B. Zhu and H. Tsang, "High coupling efficiency silicon waveguide to metal–insulator–metal waveguide mode converter," Journal of Lightwave Technology, 34(10), 2467-2472 (2016).
[14] C. Chen and et al, "Design of highly efficient hybrid Si-Au taper for dielectric strip waveguide to plasmonic slot waveguide mode converter," Journal of Lightwave Technology, 33(2), 535-540 (2015).
[15] S. Molesky and et al, "Inverse design in nanophotonics," Nat. Photonics 12, 659-670 (2018).
[16] T. Zhang and et al, "Efficient spectrum prediction and inverse design for plasmonic waveguide systems based on artificial neural networks," Photonics Research 7(3), 368-380 (2019).
[17] T. W. Hughes and et al, "Adjoint method and inverse design for nonlinear nanophotonic devices," ACS Photonics 5, 4781-4787 (2018).
[18] T. Zhang and et al, "Inverse design and optimization of graphene metamaterial for multi-peak plasmon induced transparency based on machine learning and evolutionary algorithms," arXiv:1908.01354 (2019).
[19] B. Shen and et al, "An integrated-nanophotonics polarization beamsplitter with 2.4 × 2.4 μm^2 footprint," Nat. Photonics 9, 378-382 (2015).
[20] T. Zhang and et al, "Efficient training and design of photonic neural network through neuroevolution," arXiv:1908.08012 (2019).
[21] L. Chuang and et al, "Improved binary PSO for feature selection using gene expression data," Comput. Biol. Chem. 32(1), 29-38 (2008).
[22] S. Kirkpatrick and et al, "Optimization by Simulated Annealing," Science 220(4598), 671-680 (1983).